Journal of Magnetic Resonance **154,** 136–141 (2002)
doi:10.1006/jmre.2001.2467, available online at http://www.idealibrary.com on IDEAL®

COMMUNICATIONS

Sample Restriction Using Radiofrequency Field Selective Pulses in High-Resolution Solid-State NMR

Patrick Charmont, Dimitris Sakellariou, and Lyndon Emsley[1]

Laboratoire de Stéréochimie et des Interactions Moléculaires, UMR-5532 CNRS/ENS, Ecole Normale Supérieure de Lyon, 69364 Lyon, France

Received April 2, 2001; revised August 7, 2001

In this article a method is suggested for restricting a sample (spatial localization) by preparing the magnetization with a phase-modulated radiofrequency pulse which inverts magnetization only over a very narrow range of radiofrequency field strengths. This is the most efficient method, in terms of sensitivity, of restricting the sample to improve rf homogeneity. The method is demonstrated by using it to improve the resolution obtained in a homonuclear dipolar decoupling experiment.

INTRODUCTION

Many different types of multiple-pulse sequences are now used in solid-state NMR, ranging from heteronuclear recoupling to homonuclear decoupling, and including virtually all of the possibilities in between (*1–5*). The major weakness of many of these sequences is their sensitivity to the inhomogeneity of the radiofrequency field (i.e., the radiofrequency (rf) field is not uniform over the whole sample volume). This is a classic problem in NMR, and in liquid-state NMR the main way of dealing with rf inhomogeniety has been to develop sequences that are less sensitive to the precise rf field strength (*6, 7*). In solid-state NMR this approach, although possible, is not quite as straightforward, since the sequences must also be robust with respect to the relatively large (compared to the rf) dipolar couplings and/or carbon offset frequencies. Indeed, while a few sequences (for proton–proton dipolar decoupling) have been proposed that are less sensitive to rf inhomogeneity (*7–9*), nevertheless the usual approach to avoiding this problem in solid-state NMR is to restrict the sample to a small volume in the center of the magic angle spinning (MAS) rotor.

Sample restriction suffers from three main handicaps. First, it reduces the intrinsic sensitivity of the experiment, making it realistically useful only for proton NMR (though in principle it would also improve the performance of, for example, carbon–carbon recoupling experiments, the method presented here can be placed as a building block before any ^{1}H or rare-spin NMR sequence). Second, ideally the plastic inserts typically used to restrict the sample should be susceptibility matched to the sample. In reality this is rarely the case, so that the inserts themselves induce some line broadening. Finally, it is experimentally inconvenient to pack rotors with inserts.

Recently we have proposed a method that uses static magnetic field gradients to excite magnetization in MAS experiments only in the center of the sample (*10*). This method, which is based on principles borrowed from magnetic resonance imaging, effectively removes the need for inserts, and allows the spectroscopist to choose interactively the degree of sample restriction necessary to achieve the required performance. It also avoids altogether problems of susceptibility matching. However, to implement the method one needs a CPMAS probe equipped with a gradient coil (which is currently a serious drawback), and at the current state of the art the gradients generated in such probes are not particularly strong, leading to problems with offset effects. Also, one should note that (as illustrated by the field map of Fig. 1a) while restriction of the volume to the center of the rotor does improve homogeneity, it is not the most efficient way to do so. In fact the most efficient way to improve homogeneity would be to select a volume of the sample defined by the contour lines in Fig. 1b. In this article we suggest a method for doing this by preparing the magnetization with a phase-modulated radiofrequency pulse which inverts magnetization only over a very narrow range of radiofrequency field strengths. This is the most efficient method, in terms of sensitivity, of restricting the sample to improve rf homogeneity. The method is demonstrated by using it to improve the resolution obtained in a homonuclear dipolar decoupling experiment.

RF FIELD INHOMOGENEITY

In the following we will use a model for the rf field distribution inside the coil to illustrate the ideas we shall develop. The model we use is relatively simple, and more sophisticated models exist, but the actual distribution is not important for the following

[1] To whom correspondence should be addressed: E-mail: Lyndon.Emsley@ens-lyon.fr.

1090-7807/02 $35.00

discussion, since we do not need to know the field distribution for the method to work (indeed this is possibly the most important feature of our method).

The magnetic field created by an infinitely long solenoid with "jointed turns" would be constant (i.e., perfectly homogeneous). However, the coil in a CPMAS probe usually has a relatively short length compared to the radius, and does not have jointed turns. Thus, the magnetic field it creates is inhomogeneous; that is it depends on the position inside the coil. For example, using an idealized model (*11*) we obtain

$$\mathbf{B}(M) = \int_{P \in \text{coil}} \frac{\mu_0 \mathbf{J} \wedge P\mathbf{M}}{4\pi PM^3},$$

where **J** is the current flux and P a point in the coil. We can evaluate this expression numerically to obtain the distribution shown in Fig. 1a. In the figure, each contour line corresponds to a given value of the B_X field. Analytical calculations (not developed here) show how the field changes rapidly along the coil axis and more slowly in the radial direction (perpendicular to the coil axis).

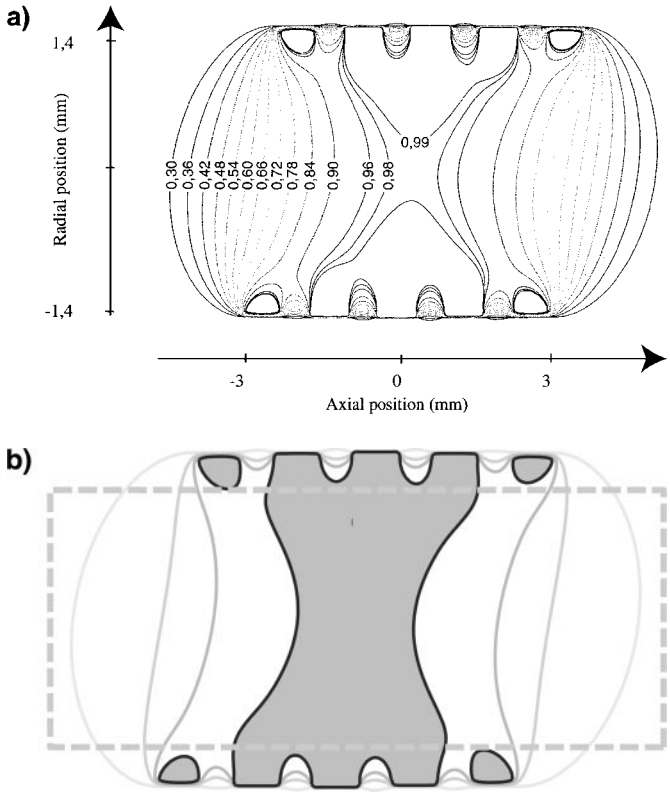

FIG. 1. (a) Simulated rf field distribution generated by the coil. The field lines do not have a simple form due to the spaces between turns. The coil has a length of 6 mm and a radius of 1.4 mm with 5 turns. The rotor used in the experiments described in the text measures 9 mm with an external radius of 1.25 mm. (b) Sample volume selected by the BISON-1 pulse described in the text. This volume corresponds to quarter of the total volume.

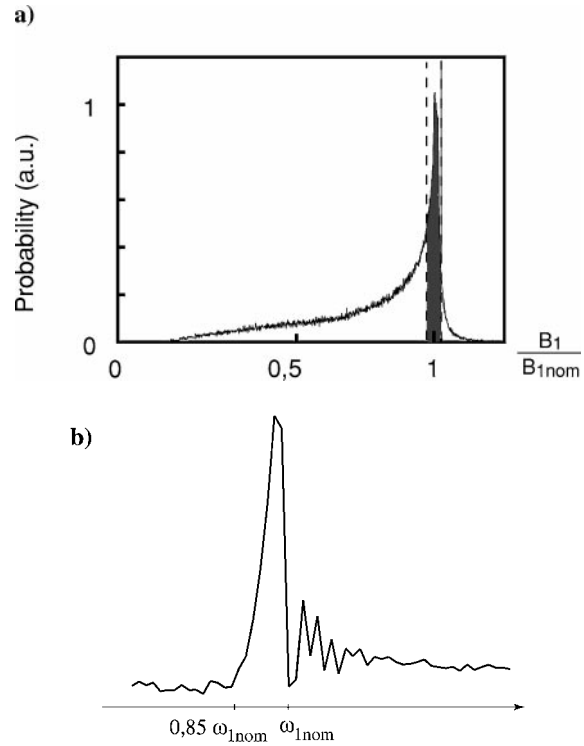

FIG. 2. (a) Simulated probability distribution of rf fields generated by the coil of Fig. 1. The probability is calculated by subdividing the space between the turns of the coil in small elementary volumes, and counting those where the field has the same value, with a given uncertainty. The shaded region indicates the range of 0.98 to 1.02 selected by the BISON-1 pulse described in the text. (b) Experimental probability distribution measured with the nutation experiment on a sodium acetate sample for a nominal rf field of around 100 kHz. The oscillations in the signal to the right of the nominal value are probably due to experimental artifacts, although we cannot explain their origin.

In Fig. 2 we show the field distribution for the coil calculated from Fig. 1a. We can see that the highest field is the most probable, but that other fields are significant for up to around 20% lower than the maximum field. This value is actually reached slightly outside the coil, but even these positions are relevant because the rotor is actually longer than the coil. The distribution shown in Fig. 2b corresponds to the distribution that can be measured experimentally using a nutation experiment. The figure corresponds to a nutation experiment performed on the carbon channel of our double-tuned Bruker 2.5-mm DVT-CPMAS probe. It can be appreciated that it contains all the essential features of the predicted distribution of Fig. 2a. Thus, it appears reasonable to assume that in a normal CPMAS probe there is an inhomogeneity of about 20%.

RADIOFREQUENCY FIELD SELECTIVE PULSES

To select only those parts of the sample that experience a particular rf field strength we propose to use the preparation sequence outlined schematically in Fig. 3a. A pulse is applied

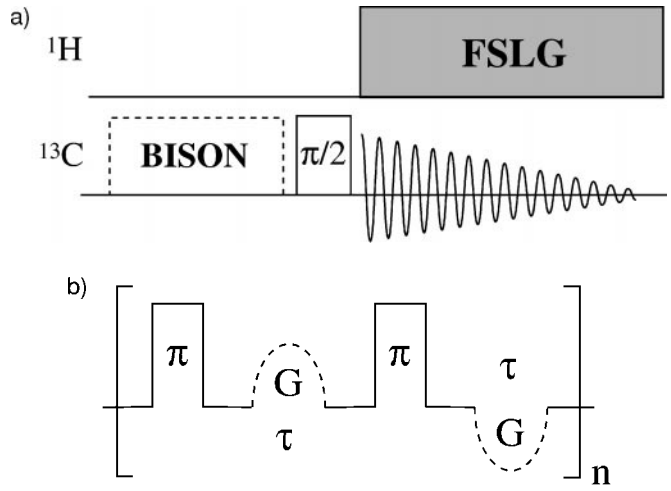

FIG. 3. (a) Pulse sequence used in the experiments presented here (available on our web site http://www.ens-lyon.fr/STIM/NMR). As the selective pulse is an inversion pulse, a $\pi/2$ pulse is used to acquire a signal. The ν_1^C field for the carbon inversion pulses was about $\nu_1^C = 100$ kHz; the FSLG decoupling was also calibrated with $\nu_1^H = 100$ kHz. Data were acquired on a 2.5-mm CPMAS probe (Bruker Avance DSX 500-MHz spectrometer). (b) Selective $(\pi - \tau)_n$ pulse, which can be used instead of BISON in the previous sequence.

which inverts magnetization only over a very narrow range of rf field amplitudes, and signal is acquired in a difference experiment with and without the field selective pulse. We are by no means the first to consider radiofrequency field selective pulses (*12–25*), which form the basis of many methods for magnetic resonance imaging using surface coils. However, existing methods do not have the required selectivity for our application, where we wish to invert magnetization over a range of only 4% of the nominal maximum rf field strength in a quite selective fashion. (Clearly, a pulse that inverts a region of 20% around the nominal maximum fields will, in our probes, select the whole sample!) Notably, in order to apply our experiment to achieve sample restriction in a way similar to that achieved by using inserts, we wish to select a square profile for the B_1 distribution instead of a Gaussian one. Thus, we have derived a new pulse scheme particularly suitable for sample restriction applications in solid-state NMR. To do this we have adopted an approach using phase-modulated pulses analogous to the so-called DUMBO approach we have recently introduced for homonuclear dipolar decoupling sequences (*8*). We should note, however, that some of the existing B_1 selective pulses may also be promising in this context, with the family of pulses suggested by Shaka and Freeman (*17–19*) (which yield a roughly Gaussian profile) appearing relatively attractive (though we have not tested their performance experimentally). Our objective here is not to compare different selective pulses, but rather to demonstrate that this approach is of use to improve resolution in solid-state NMR experiments.

This approach (which has previously been applied to a range of problems in NMR (*6, 9*)) consists in the numerical optimization of the simulated NMR response to a pulse which is defined by an arbitrary function with many variable parameters. We use a representation of the phase of the pulse in terms of a Fourier series

$$\varphi = \sum_{n=1}^{N} a_n \cos\left(n\frac{2\pi}{\tau}t\right) + b_n \sin\left(n\frac{2\pi}{\tau}t\right) \quad (0 \le t \le \tau),$$

where τ is the length of the pulse. The amplitude of the pulse is constant. We have chosen a Fourier series since it represents a convenient basis set of functions (and it yields satisfactory results), but in principle any other basis functions could be used. The optimization procedure consists in finding an optimal set of the Fourier coefficients a_n and b_n. For purely practical reasons of computational time, the Fourier series is truncated at 10th order, yielding an optimization using 20 variable parameters. Also, for practical reasons the pulse must be "discretized," yielding

$$\Delta t = \frac{\tau}{M} \Rightarrow \varphi = \sum_{n=1}^{N} a_n \cos\left(2\pi\frac{np}{M}\right) + b_n \sin\left(2\pi\frac{np}{M}\right)$$
$$\text{if } (p-1)\Delta t \le t \le p\Delta t.$$

For each set of coefficients the response of an isolated single spin, neglecting magic angle spinning, is evaluated numerically as a function of the rf field amplitude, ω_1, using the Bloch equations, where for each step in the pulse, the evolution is given by

$$\begin{pmatrix} M_x' \\ M_y' \\ M_z' \end{pmatrix} = [T] \begin{pmatrix} M_x \\ M_y \\ M_z \end{pmatrix}$$

with

$$[T] = \begin{bmatrix} \cos\theta + \cos^2\varphi(1-\cos\theta) & \cos\varphi\sin\varphi(1-\cos\theta) & \sin\varphi\sin\theta \\ \cos\varphi\sin\varphi(1-\cos\theta) & \cos\theta + \sin^2\varphi(1-\cos\theta) & -\cos\varphi\sin\theta \\ -\sin\varphi\sin\theta & \cos\varphi\sin\theta & \cos\theta \end{bmatrix},$$

where $\theta = \omega_1 \Delta t$.

The quality of the response is then determined by least-squares comparison with a target function. The target function we used in the optimization procedure is shown in Fig. 4. The optimization was started by generating several million random sets of Fourier coefficients and evaluating the quality factor. The best 10 sets were then used as starting points in a least-squares gradient descent method (the MINUIT method). The performance of our best result so far is shown in Fig. 4, and the Fourier coefficients for this pulse are given in Table 1. To obtain a pulse having a sufficiently square response requires the use of at least 10 Fourier coefficients. (No dependence of these coefficients on the radiofrequency field strength has been observed.) We dub this pulse BISON-1 (B_1 is selected by optimizing numerically). As can be seen from the figure, BISON-1 inverts magnetization

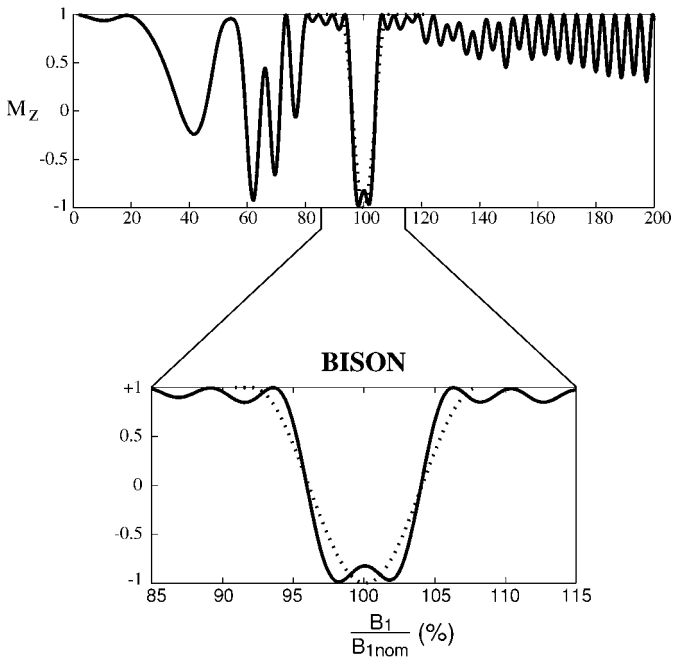

FIG. 4. Simulated response to the BISON-1 sequence (solid line), and the target function used in the minimization (dashed line).

only over a range of ±4% around the nominal maximum value, and leaves the following 16% untouched; the pulse does have an effect at even lower field strengths, but these should normally not be present in the sample. Figure 2 shows the predicted distribution that should be obtained with BISON-1, and Fig. 1b shows the regions of the sample within the probe that are selected by the pulse. As we mentioned above, the profile obtained with this pulse is not necessarily more "selective" than others in the literature (*12–25*), but it is more "square" and seems well adapted to the application to solid-state NMR experiments. (Curiously, we found this satisfying "square" response result using a Gaussian objective function.) In any case, we recall that our objective is to demonstrate the use of such pulses to restrict the sample, and we are not necessarily claiming that BISON-1 is "better" than any other alternative on any absolute scale.

TABLE 1
Fourier Coefficients for the BISON-1 Sequence

i	*a*	*b*
1	3.124	−9.558
2	2.738	−1.254
3	1.712	−2.259
4	1.609	−1.295
5	0.09	−1.105
6	0.769	−0.734
7	−0.434	−0.851
8	0.584	−0.413
9	−0.267	−1.189
10	1.468	−1.397

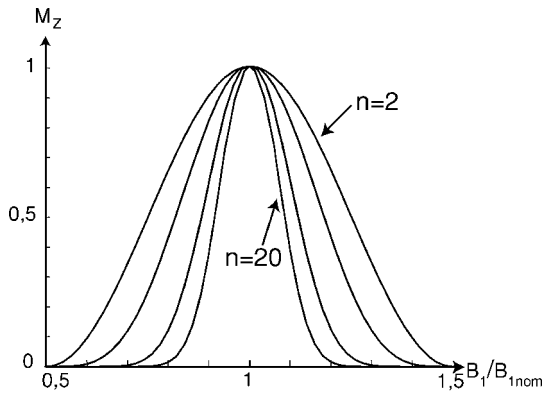

FIG. 5. Simulated B_1 inversion profile for $(\pi - \tau)_n$ sequences. The higher the n, the narrower the B_1 profile. To be useful, large values of n are necessary, so theses pulses will be efficient for a sample with a long T_1 and a short T_2, so that the transverse magnetization dephases quickly during a short τ delay, and the signal does not disappear at large n.

Note that we have chosen to optimize an inversion pulse and use a difference scheme, rather than directly optimize a B_1 selective excitation pulse. This is because inversion is a considerably easier problem (*26*). Our attempts to find a (pure phase) B_1 selective excitation pulse have so far failed to give satisfactory results.

Finally, we remark that there is another, less demanding (but substantially longer), way of achieving B_1 selective inversion which is shown in Fig. 3b. This sequence consists of a train of ordinary π pulses followed by dephasing delays (or gradients). As the number of π pulse increases (where the total number of π pulses is even), the selectivity of inversion increases accordingly as shown in Fig. 5.

As shown below, both approaches appear to work experimentally, and the choice between the two probably depends on the details of the particular experimental setup and the sample.

APPLICATION TO HOMONUCLEAR DIPOLAR DECOUPLING EXPERIMENTS

As an illustrative example we have applied both kinds of inversion pulses to a sample of polycrystalline sodium acetate in a Bruker 2.5-mm double-tuned DVT-CPMAS probe using the sequences shown in Fig. 3a. During acquisition we observe the carbon-13 signal in the presence of FSLG (*27*) homonuclear dipolar decoupling applied to the protons. As we have demonstrated previously (*4*), the resolution of the fine structure due to the carbon–proton heteronuclear scalar coupling is a direct indicator of the performance of the homonuclear proton–proton dipolar decoupling. The FSLG sequence is known to be sensitive to rf inhomogeneity, so we expect to see an improvement of the performance of the sequence when we restrict the sample to a small range of B_1 fields.

The results obtained using the $(\pi - \tau)_n$ sequence are shown in Fig. 6 in which we show the methyl group quartet as a function of n with and without FSLG. The spectra without FSLG show that as n increases the signal diminishes since the range of

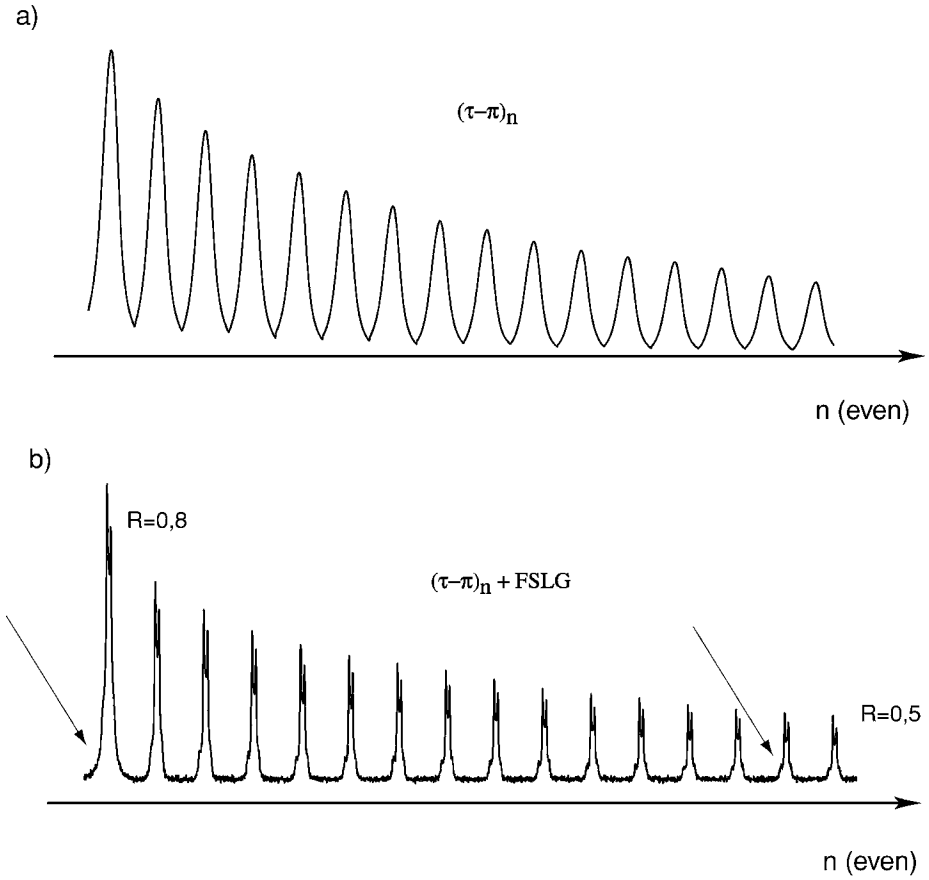

FIG. 6. (a) Experimental performance of $(\pi - \tau)_n$ preparation sequences obtained using the sequence of Fig. 3b for the carbon-13 signal of sodium acetate. (a) Methyl resonance of sodium acetate acquired without FSLG decoupling. As n increases the width of the selected B_1 distribution decreases, and therefore the excited volume is reduced. (b) With FSLG homonuclear proton–proton decoupling during acquisition (with $\nu_1^C \simeq 100$ kHz), the quartet fine structure due to the heteronuclear ^{13}C–^{1}H J coupling is better and better resolved as inhomogeneity decreases. We note that a value $n \sim 20$ yields high-quality decoupling without too much signal loss. R is defined as the intensity ratio of the lowest to the highest part of the doublet and defines the "resolution" of the doublet. The arrows highlight how the outer transitions of the methyl quartet also become better resolved with increasing n. A τ value of 150 ms was used and found to be the shortest compatible with dephasing of the transverse magnetization. This delay could be considerably reduced by using B_0 field gradients to dephase the magnetization during the τ period.

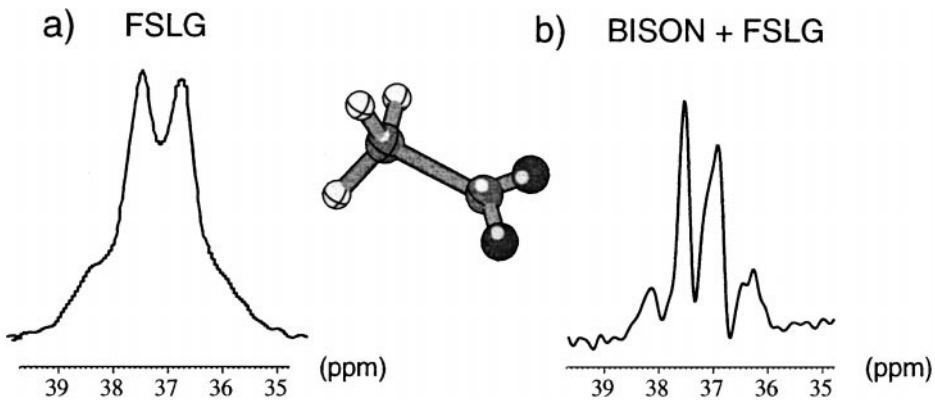

FIG. 7. (a) Methyl quartet of sodium acetate decoupled without BISON. The linewidth is around 100 Hz and we can barely see the outer lines. (b) Quartet decoupled with FSLG and prepared with BISON-1. The linewidth is now around 30 Hz and we can distinguish the four lines of the quartet. 320 scans were acquired for each of the spectra. The rf fields were as in Fig. 6, and the BISON-1 pulse was implemented as 640 steps of 300 ns duration for a total pulse length of 192 μs at a ν_1^C of 100 kHz. (BISON-1 is a 40π on-resonance pulse.)

selected values of B_1 becomes smaller and smaller. Accordingly, as expected, the series of spectra with homonuclear decoupling shows increasing resolution as n is increased. Optimum resolution is achieved when n is around 16, where we have selected the most homogeneous 30% of the sample. Although this may lead to long preparation sequences (2.4 s for $n = 16$ without gradients to dephase the signal during the τ periods), this figure highlights the flexibility of this approach which allows one to determine interactively the sample restriction required to obtain optimum performance. This allows the spectroscopist to find the best compromise between signal-to-noise requirements and pulse sequence efficiency.

Figure 7 shows the methyl group quartet under FSLG proton decoupling with and without BISON-1. Since the width of the B_1 interval selected by the pulse is very narrow (4% of the maximum B_1 value) the rf field is very homogeneous and leads to exceptionally good decoupling. The full width at half-height of one of the inner components of the methyl quartet is $\sim$30 Hz, corresponding to a gain of a factor 3 in resolution in this case.

CONCLUSION

We have introduced two ways to restrict the sample in solid-state NMR to only those parts that experience the same (to within a given degree) radiofrequency field amplitude. The simplest method involves a series of π pulses. A more sophisticated approach makes use of a numerically derived phase-modulated B_1 selective inversion pulse, dubbed BISON-1. Both approaches are shown to work well, with the BISON-1 method yielding a factor 3 improvement in resolution in an experiment involving proton–proton homonuclear decoupling.

These new spectroscopic sample restriction techniques can be implemented on any existing probe or spectrometer, and we expect them to replace physical inserts.

REFERENCES

1. H. Geen, Theoretical design of amplitude-modulated pulses for spin decoupling in nuclear magnetic resonance, *J. Phys. B: At. Mol. Opt. Phys.* **29,** 1699–1710 (1996).
2. J. S. Waugh, L. M. Huber, and U. Haeberlen, Approach to high-resolution NMR in solids, *Phys. Rev. Lett.* **20,** 180–182 (1968).
3. D. P. Burum and W. K. Rhim, Analysis of multiple pulse NMR in solids, *J. Chem. Phys.* **71,** 944–956 (1979).
4. D. P. Burum, M. Linder, and R. R. Ernst, Low-power line narrowing in solid-state NMR, *J. Magn. Reson.* **44,** 173–188 (1981).
5. A. E. Bennett, R. G. Griffin, and S. Vega, Recoupling of homo- and heteronuclear dipolar interactions in rotating solids, *NMR Basic Principles Prog.* **33,** 1–77 (1994).
6. J. Baum, R. Tycko, and A. Pines, Broadband population inversion by phase modulated pulses, *J. Chem. Phys.* **79,** 4643–4644 (1983).
7. M. H. Levitt, "The Encyclopedia of NMR," Wiley, London (1997).
8. D. Sakellariou, A. Lesage, P. Hodgkinson, and L. Emsley, Homonuclear dipolar decoupling in solid-state NMR using continuous phase modulation, *Chem. Phys. Lett.* **319,** 253–260 (2000).
9. Y. Ishii and T. Terao, Manipulation of nuclear spin hamiltonians by rf-field modulations and its applications to observation of powder patterns under magic-angle spinning, *J. Chem. Phys.* **109,** 1366–1374 (1998).
10. P. Charmont, A. Lesage, S. Steuernagel, F. Engelke, and L. Emsley, Sample restriction using magnetic field gradients in high-resolution solid-state NMR, *J. Magn. Reson.* **145,** 334–339 (2000).
11. J. D. Jackson, "Classical Electrodynamics," Wiley, New York (1998).
12. P. G. Morris, "Nuclear Magnetic Resonance Imaging in Medicine and Biology," Clarendon, Oxford (1986).
13. R. Tycko and A. Pines, Spatial Localization of NMR signals by narrowband inversion, *J. Magn. Reson.* **60,** 156–160 (1984).
14. R. Kemp-Harper, P. Styles, and S. Wimperis, B_1-selective pulses, *J. Magn. Reson. A* **123,** 230–236 (1996).
15. A. J. Shaka and A. Pines, Symmetric phase-alternating composite pulses, *J. Magn. Reson.* **71,** 495–503 (1987).
16. K. Scheffler, Design of B_1-insensitive and B_1-selective RF pulses by means of stochastic optimization, *J. Magn. Reson. B* **109,** 175–183 (1995).
17. A. J. Shaka, J. Keeler, M. B. Smith, and R. Freeman, Spatial localization of NMR signals in an inhomogeneous radiofrequency field, *J. Magn. Reson.* **61,** 175–180 (1985).
18. A. J. Shaka and R. Freeman, A composite 180° pulse for spatial localization, *J. Magn. Reson.* **63,** 596–600 (1985).
19. A. J. Shaka and R. Freeman, "Prepulses" for spatial localization, *J. Magn. Reson.* **64,** 145–150 (1985).
20. S. Wimperis, Broadband, narrowband, and passband composite pulses for use in advanced NMR experiments, *J. Magn. Reson. A* **109,** 221–231 (1994).
21. D. I. Hoult, The solution of the Bloch equations in the presence of a varying B_1 field—An approach to selective pulse analysis, *J. Magn. Reson.* **35,** 69–86 (1979).
22. C. J. Hardy and H. E. Cline, Spatial localization in two dimensions using NMR designer pulses, *J. Magn. Reson.* **82,** 647–654 (1989).
23. C. G. Malloy, R. A. Lange, D. L. Klein, F. M. Jeffrey, R. M. Peshock, J. T. Willerson, and R. L. Nunnally, Spatial localization of NMR signal with a passive surface gradient, *J. Magn. Reson.* **80,** 364–369 (1988).
24. D. Canet, D. Boudot, A. Belmajdoub, A. Retournard, and J. Brondeau, Accurate spatial localization by a novel sequence using a RF field gradient and a DANTE-like pulse train, *J. Magn. Reson.* **79,** 168–175 (1988).
25. M. G. Crowley and J. J. H. Ackerman, Enhanced surface-coil spatial localization with an inhomogeneous surface gradient, *J. Magn. Reson.* **65,** 522–525 (1985).
26. L. Emsley, Selectives pulses, *in* "Encyclopedia of NMR," Wiley, London (1996).
27. A. Bielecki, A. C. Kolbert, and M. H. Levitt, Frequency-switched pulses sequences: Homonuclear decoupling and dilute spin NMR in solids, *Chem. Phys. Lett.* **155,** 341–346 (1989).